AFRL-SR-AR-TR-02-0163

(TECHSAT 21) Advanced Ionospheric Effects Sensor – Research and Development

M. Alvin Morgan
AMPTEK

April 30, 2002

Air Force Research Laboratory
Air Force Office of Scientific Research
Arlington, Virginia

REPORT DOCUMENTATION PAGE

AFRL-SR-AR-TR-02-

0163

1. AGENCY USE ONLY *(Leave blank)*	2. REPORT DATE	3. REPO
		01 February 1999 - 31 January 2002

4. TITLE AND SUBTITLE
(TECHSAT 21) Advanced Ionospheric Effects Sensor - Research and Development

5. FUNDING NUMBERS
F49620-99-C-0008

6. AUTHOR(S)
M. Alvin Morgan

7. PERFORMING ORGANIZATION NAME(S) AND ADDRESS(ES)
AMPTEK
6 DeAngelo Drive
Bedford, MA 01730-2204

8. PERFORMING ORGANIZATION REPORT NUMBER

9. SPONSORING/MONITORING AGENCY NAME(S) AND ADDRESS(ES)
AFOSR/NM
801 N. Randolph Street Room 732
Arlington, VA 22203-1977

10. SPONSORING/MONITORING AGENCY REPORT NUMBER
F49620-99-C-0008

11. SUPPLEMENTARY NOTES

12a. DISTRIBUTION AVAILABILITY STATEMENT
APPROVED FOR PUBLIC RELEASE, DISTRIBUTION UNLIMITED

12b. DISTRIBUTION CODE

13. ABSTRACT *(Maximum 200 words)*

A good deal of effort was put into analyzing the anticipated instrument (DIDM-3) performance. the instrument design, using a backgammon type anode and four charge amps, was looked-at to determine: (1) if a design can be produced which provided optimal performance, and (2) whether the design provides adequate imaging resolution for the drift measurements. The design optimization efforts were reported on in a previous report, and in the subsequent material the following analysis are presented: (1) expected measurement accuracy and resolution; (2) count rate effects on performance.

14. SUBJECT TERMS	15. NUMBER OF PAGES
	14
	16. PRICE CODE

17. SECURITY CLASSIFICATION OF REPORT	18. SECURITY CLASSIFICATION OF THIS PAGE	19. SECURITY CLASSIFICATION OF ABSTRACT	20. LIMITATION OF ABSTRACT

AFOSR BAA-PR3

(TECHSAT 21) ADVANCED IONOSPHERIC EFFECTS SENSOR-RESEARCH AND DEVELOPMENT

AMPTEK, INC.
6 De Angelo Drive
Bedford, Massachusetts 01730

30 April 2002

Final Report
01 January 1999 through 01 January 2002

Contract #F49620-99C-0008

Distribution:

AFOSR/NM
DCMAO/ACO
AFOSR/PK3

Prepared for:

AIR FORCE OFFICE OF SCIENTIFIC RESEARCH
Directorate of Mathematics and Space Sciences
801 N. Randolph Street, Room 732
Arlington, VA 22203-1977

Contents

Section		Page
1.0	INTRODUCTION	1
2.0	SUMMARY OF ACTIVITIES	1
3.0	MEASUREMENT ACCURACY AND RESOLUTION	1
3.1	Requirements and Objectives	1
3.2	Ion Drift Determination	2
3.3	Thermal Spreading	3
3.4	Individual Interaction Locations	3
3.5	Electronic Noise	4
3.6	Charge Fluctuation Effects	6
3.7	Anode Resolution	6
3.8	Anode Optimization	7
4.0	COUNT RATE EFFECTS	8
4.1	Count Rate Calculations	8
4.2	Low Count Rate Considerations	9
4.3	High Count Rate Pile-up Considerations	9

List of Figures

Number		Page
1	Sketch of Backgammon Anode Concept	4
2	MCP Count Rate vs. Density	8
3	Histogram of: (a) Counts vs. Azimuth; (b) Counts vs. Elevation; without pile-up (in blue) and with 25% pile-up (in red), for T=1,000 K	10

List of Tables

Number		Page
1	Table of DIDM Requirements and Objectives	2
2	Table of Required Angular Resolution for Locating Centroid of a Thermally Distributed Ion Population	3
3	Pile-up Fraction at 3 Temperatures for Elevation and Azimuth	10
4	Count Rate Effect Summary	11

1.0 INTRODUCTION

This is the third and final status report for contract # F49620-99C-0008. The contract's objective is to carry out research and development studies on a small size, low power, low weight, space plasma diagnostic instrument suite, to facilitate scientific studies of ionospheric structures which develop in both the magnetic equator and polar cap regions of the earth, that could seriously compromise the performance of space-based radar systems. Ultra-high resolution, spatial and temporal characterization data for these structures must be obtained, so that the physics of their formation might be understood, their impact on electromagnetic propagation assessed and operational measures to counter their effect developed.

Furthermore, the devices will be of the enhanced performance type and satisfy operating requirements that are near the limit of what is practically realizable.

2.0 SUMMARY OF ACTIVITIES

A good deal of effort was put into analyzing the anticipated instrument (DIDM-3) performance. The instrument design, using a backgammon type anode and four charge amps, was looked-at to determine: (1) if a design can be produced which provided optimal performance, and (2) whether the design provides adequate imaging resolution for the drift measurements. The design optimization efforts were reported on in a previous report, and in the subsequent material the following analysis are presented: (1) expected measurement accuracy and resolution; (2) count rate effects on performance.

3.0 MEASUREMENT ACCURACY AND RESOLUTION

3.1 Requirements and Objectives

Based on the provided inputs from AFRL, the requirements for the instrument are summarized in Table 1. The environmental objectives for DIDM derive from two sources, NPOESS EDRs (Environmental Data Records) and C/NOFS objectives. Each constitute a challenging set of requirements and combining them does not make the task at hand any easier. Due to the statistical limitations of the instrument, it is difficult to match a realistic DIDM specification to a single requirement, and it is generally more useful to use the two instrument parameters of precision and count rate.

The specifications are taken from requirements put out by the NPOESS, C/NOFS, and TechSat programs. NPOESS lists both a "threshold level" and an "objective level", where the objective level is more stringent. It is necessary to meet the threshold level and desirable to meet the objective level as well.

A resolution for the drift measurement is not listed explicitly in Table 1. NPOESS does not appear to specify a spatial resolution for this measurement. It is known that AFRL theorists desire a spatial resolution of 3.5 meters for C/NOFS, but the Principal Investigator (PI) has indicated that a reasonable objective would be 200 m with a precision of 25 m/sec, and the capability to measure the drift more frequently with an attendant loss of precision. Note that in some requirements both precision and accuracy are separately called out, while in other requirements only one is given. It is understood that precision refers to random fluctuations in repeated, identical measurements while accuracy refers to errors due to systematic effects. Where these are not separately specified, it is assumed that the total combination of the two is the intended quantity. It is also assumed that these quantities are all specified in terms of "rms" rather than "FWHM"

Table 1. Table of DIDM Requirements and Objectives

		NPOESS Specification	NPOESS Objective	C/NOFS Objective	TechSat Objective
Drift Velocity	Range (km/sec)	0 to 3	0 to 5		
	Precision (m/sec)	50	25	10	
	Accuracy (m/sec)	75	50	10	
Plasma Density	Range (cm^{-3})	$5x10^3$ - $5x10^6$	10^2-10^7		
	Accuracy	20%	5%	1%	
	Resolution (km)	50	10	1	0.01
Plasma Temperature	Range (°K)	500 to 10,000			
	Accuracy	10%	5%		
	Resolution (km)	100	10 km		
Plasma Fluctuations	Resolution (km)	100	10		0.01
	$\Delta N/N$	10^{-2} to 1	10^{-4} to 1		
	Precision of $\Delta N/N$	Greater of 20% or 10^4 cm^{-3}	5% or $2x10^2$ cm^{-3}		

3.2 Ion Drift Determination

To determine the drift velocity, we determine the centroid of a distribution of incident ions. We are not interested in the ability to locate one interaction, but in the ability to locate a centroid. Assume that the 10 m/sec velocity is orthogonal to the spacecraft ram, which is 7.2 km/sec. This implies a polar angular resolution of:

$$\theta = \tan^{-1}\left(\frac{10}{7200}\right) = \tan^{-1}\left(1.39\times10^{-3}\right) = 0.08^\circ$$

The 35° total range corresponds to 4.4 km/sec, close to the NPOESS objective. The necessary azimuthal resolution depends upon the polar angle, i.e. on the component of drift velocity orthogonal to ram. For a 1 km/sec drift the polar angle is 8°. To detect a 10 m/sec change in velocity perpendicular to this, in the ram direction, we have to detect a change in azimuthal angle of:

$$\phi = \tan^{-1}\left(\frac{0.01}{1}\right) = 0.6^\circ$$

At a lower drift velocity, the angular resolution decreases, i.e. to 1.1° at 4° polar angle. At higher drift velocities the required azimuthal angular resolution increases. At the limit, 4.4 km/sec, 10 m/sec corresponds to 0.13°. This corresponds to 0.04% azimuthal resolution, at the outer limit.

As will be shown in the next section, thermal spreading will cause individual ions to be distributed over a much larger angular range than these values. To located the centroid this accurately will require two things: (1) enough counts in the distribution, since the uncertainty in the mean of a distribution is lower than the spread of a distribution, by 1/N, and (2) systematic errors in the anode imaging capability that, when averaged over the region of a typical thermal distribution, are below the levels shown in Table 2.

Table 2. Table of Required Angular Resolution for Locating Centroid of a Thermally Distributed Ion Population

	10 m/sec	25 m/sec	50 m/sec
Elevation	0.08°	0.2°	0.4°
Azimuth	0.13°	0.33°	0.6°

3.3 Thermal Spreading

The following MathCad worksheet computes the rms spreading in angle due to the various thermal distributions. It is based upon simple geometry: the rms velocity in a single component is

$k := 1.381 \cdot 10^{-16} \cdot \frac{erg}{K}$ $M_A := 16$ $m := 1.67 \cdot 10^{-24} \cdot gm$

Incident angle which maps to outer edge of anode $\phi_{max} := 35 \cdot \left(\frac{\pi}{180} \right)$

$T_{min} := 500$ $T_{max} := 10 \cdot 10^3$ $T_{avg} := 1600$

RMS Thermal Speed for one component (cm/s) (Bittencourt, p 177, Eqn 4.8) $v_{xrms}(T) := \sqrt{\frac{k \cdot T \cdot K}{M_A \cdot m}}$

$\phi_{rms}(T) := \operatorname{atan}\left(\frac{v_{xrms}(T)}{v_{ram}} \right)$ $\theta_{rms}(T, \phi) := \operatorname{atan}\left(\frac{v_{xrms}(T)}{v_{ram} \cdot \sin(\phi)} \right)$

Cold	Average	Hot
$v_{xrms}(T_{min}) = 5.084 \times 10^4 \frac{cm}{sec}$	$v_{xrms}(T_{avg}) = 9.094 \times 10^4 \frac{cm}{sec}$	$v_{xrms}(T_{max}) = 2.273 \times 10^5 \frac{cm}{sec}$
$\phi_{rms}(T_{min}) \cdot \frac{180}{\pi} = 4.039$	$\phi_{rms}(T_{avg}) \cdot \frac{180}{\pi} = 7.198$	$\phi_{rms}(T_{max}) \cdot \frac{180}{\pi} = 17.524$
$\theta_{rms}(T_{min}, \phi_{max}) \cdot \frac{180}{\pi} = 7.018$	$\theta_{rms}(T_{avg}, \phi_{max}) \cdot \frac{180}{\pi} = 12.418$	$\theta_{rms}(T_{max}, \phi_{max}) \cdot \frac{180}{\pi} = 28.833$

taken to be orthogonal to the ram or to a combination of ram and drift.

So the smallest distribution that will ever be observed has an rms fluctuation of 4° in elevation and 7° in azimuth. To achieve 10 m/sec precision or accuracy requires 0.08° and 0.13°, respectively, or a centroid location that is 50-55 times more accurate than the spreading in the incident distribution.

3.4 Individual Interaction Locations

How well should we be able to locate a single ion? More explicitly, what should be the accuracy and precision with which we can locate the centroid of a single charge cloud exiting the MCP from a single incident ion? The PI at AFRL has indicated that we should aim for 1%. This implies 0.35° in elevation and 3.6° in azimuth.

If the imaging resolution of the anode and electronics are poor, then the centroid of the measured distribution will still be accurate. This does not degrade the resolution with which we can

ultimately measure the ion drift. However, there will be two negative consequences: (1) it will take a longer time to acquire the necessary counts to measure the centroid accurately, and (2) the apparent excessive width will increase the temperature that is determined from the synthetic aperture technique.

Note that the imaging resolution of the anode and electronics adds in quadrature to the thermal distribution. It is conceivable that an acceptable resolution would be 50% of the very worst-case thermal distribution. We can therefore tolerate 2° imaging resolution in elevation and 3.5° in azimuth. This azimuthal requirement corresponds to the instrument adding <10% broadening for a 500K thermal distribution with a 4.5 km/sec ion drift - the worst possible combination of parameters.

3.5 Electronic Noise

A sketch of the backgammon concept is shown in Figure 1. An incident charge Q is deposited over a small region at some location. The charge is divided between the four charge amps, with the division depending on location. The azimuthal charge division is based on the aspect ratio of the anode, while the elevation charge division is based on the capacitive divider chain. The location of the centroid of a charge cloud is determined from the four measured charges X1 through X4, in the two orthogonal axes, as:

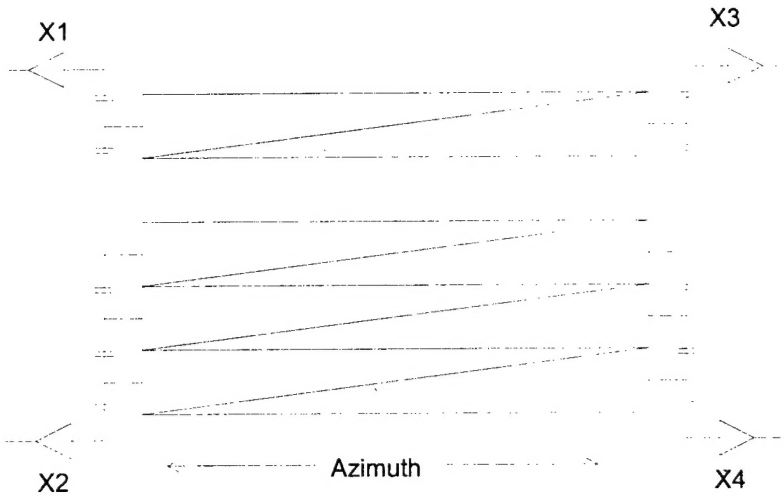

Figure 1. Sketch of Backgammon Anode Concept

$$Azimuth = \frac{(X_1 + X_2) - (X_3 + X_4)}{X_1 + X_2 + X_3 + X_4} \qquad Elevation = \frac{(X_1 + X_3) - (X_2 + X_4)}{X_1 + X_2 + X_3 + X_4}$$

There are many variants on this basic concept. In DIDM, the anode is cylindrical, thus the rectangle shown below maps into a polar geometry. The anodes can be "asymmetric", as here, or can be symmetric. The Azimuth and Elevation expressions can be differential, as here, or single-ended. All these variants are conceptually similar. It can be argued that what is presented here is the best in terms of precision and accuracy.

There will be some inevitable fluctuations in the measured charges X1 through X4, due to electronic noise and to quantum fluctuations. The goal of this section is to estimate the magnitude of these fluctuations, to see if they will degrade image resolution. Both elevation and azimuth are determined by expressions of the form:

$$A = \frac{P - M}{P + M}$$

where: P and M are the sum of two preamplifier outputs, i.e. P=X1+X2 or X1+X3, depending on the axis. With the currently planned15 wedge pairs with an aspect ratio of 15:1 (each wedge has a "tail" 1/15 the "head), P and M each cover the range of about 0.1 to 0.9 times the total charge, so A ranges from -0.8 to +0.8. The quantity "A" shown here must be scaled appropriately to give the actual range, i.e. 0° to 35° or 0° to 360°.

To get the uncertainty in A requires a bit of derivation. In general, if we have A=f(P,M) where P and M have statistically independent errors σ_P^2 and σ_M^2. Then[1]

$$\sigma_A^2 = \left(\frac{\partial f}{\partial P}\right)^2 \sigma_P^2 + \left(\frac{\partial f}{\partial M}\right)^2 \sigma_M^2$$

We have

$$f = \frac{P-M}{P+M}$$

$$\frac{\partial f}{\partial P} = \frac{1}{P+M} - \frac{P-M}{(P+M)^2} = \frac{(P+M)-(P-M)}{(P+M)^2} = \frac{-2M}{(P+M)^2}$$

$$\frac{\partial f}{\partial M} = \frac{1}{P+M} - \frac{P-M}{(P+M)^2} = \frac{-(P+M)-(P-M)}{(P+M)^2} = \frac{-2P}{(P+M)^2}$$

$$Var\left(\frac{P-M}{P+M}\right) = \left(\frac{-2M}{(P+M)^2}\right)^2 Var(P) + \left(\frac{-2P}{(P+M)^2}\right)^2 Var(M)$$

Assuming that $\sigma_P^2=\sigma_M^2$,

$$\sigma_A^2 = \left[\frac{4\left(P^2+M^2\right)}{(P+M)^4}\right]\sigma_P^2$$

Assume now that our minimum gain is $1x10^6$. We can consider two limiting cases, where P=M=0.5x106 (near the middle) and where $P=0.1x10^6$ and $M=0.9x10^6$ (or vice-versa, near either end). It is reasonable to assume that σ_P=3,000 electrons rms or less - this is a reasonable number for the electronic noise. Then:

Middle:

$$\sigma_A^2 = \left[\frac{4\left(\left(0.5\times10^6\right)^2+\left(0.5\times10^6\right)^2\right)}{\left(1\times10^6\right)^4}\right]\left(3\times10^3\right)^2 = \frac{\left(2\times10^{12}\right)\left(9\times10^6\right)}{1\times10^{24}} = 18\times10^{-6}$$

$$\sigma_A = 4\times10^{-3}$$

Ends:

$$\sigma_A^2 = \left[\frac{4\left(\left(0.1\times10^6\right)^2+\left(0.9\times10^6\right)^2\right)}{\left(1\times10^6\right)^4}\right]\left(3\times10^3\right)^2 = \frac{\left(3\times10^{12}\right)\left(9\times10^6\right)}{1\times10^{24}} = 27\times10^{-6}$$

$$\sigma_A = 5\times10^{-3}$$

Since A covers a range of -0.8 to +0.8, at all locations, the electronic noise causes <0.3% measurement uncertainty. This is assuming an electronic noise of 3,000 electrons rms, which is probably conservative - the real noise is likely to be less. This also assumes a gain of $1x10^6$. The resolution goes inversely with gain, so increasing gain will help. The gain could be lowered somewhat before electronic noise would start to become a problem.

We have previously discussed a "single-ended" measurement, using P alone in the numerator instead of P-M. The differential measurement doubles the range of A, i.e. doubles the signal. For the noise, the (P^2+M^2) in the numerator for the differential measurement becomes P^2 alone for the single-

[1] For example, see Mandel, *The Statistical Analysis of Experimental Data*, Dover Pubs, p 74

ended measurement. Basically, with a differential measurement the noise increases by about $\sqrt{2}$ while the signal doubles, so the signal to noise ratio increases by $\sqrt{2}$. The actual situation is a little more complicated, since for the single-ended measurement the noise is more dependent on position.

3.6 Charge Fluctuation Effects

In addition to electronic noise, there will be fluctuations in the output signal due to quantum charge collection effects. If the average signal is 0.25×10^6 electrons in each preamp, then assuming Poisson statistics, fluctuations on the order of 500 electrons will be seen. It is not clear however, that Poisson statistics really apply here. In some charge generation processes, there is a correlation, which reduces the fluctuations below that expected by Poisson statistics. In other processes, including all those involving avalanche gain, there is an increase in fluctuations above that expected by Poisson statistics. The essential physical origin of this "excess noise" is that the random fluctuation in the first stage of the gain process gets amplified by the subsequent gain stages. The MCP being an avalanche device, it can be expected that one would see excess noise in the gain distribution, but not necessarily in the spatial distribution. In fact, since charge cloud spreading is in part due to Coulomb repulsion - i.e. a correlated behavior - the fluctuations might be smaller than Poisson. For this first analysis, the term will be ignored.

3.7 Anode Resolution

It is also important to consider what is meant by term the "anode resolution": given ideal, noise-free electronics and no quantum fluctuations, what would be the resolution obtained from the anode? To answer this question, a MathCad model was created, in which the charge deposited on all 30 wedges was computed for a gaussian charge distribution. The wedge geometry was modeled using analytical expressions for $\rho(\phi)$ to define the wedges. It was assumed that: (1) a 1 mil tail, (2) a 15 mil head, and (3) 1 mil separations throughout. The charge distribution was modeled as a gaussian, with a σ of 10, 15, and 20 mils. MathCad computed the numerical integrals of the gaussian charge distribution between the radial and angular limits defined by the wedges. A random number generator was used to select incident locations uniformly distributed over the anode. Some important results were as follows:

1. There exists a systematic distortion: the measured elevation depends on azimuth, with a change of 1 mil over the full 360°.

   1.1. This distortion is due to the 1 mil separation between each pair of wedges: the measurement of (X1+X2)-(X3+X4) compares the position of the spot to the average of the two, and since X1 and X2 are offset from X3 and X4 by the 1 mil separation, the apparent location moves by 1 mil. If you fix a charge cloud centroid at a radial position in the middle of a wedge pair and change azimuth by 360°, then the apparent radial position varies between $\pm$0.5 mil.

   1.2. Assuming that we use about 200 mils of the anode, this is a 0.25% effect, a 0.9° effect, i.e. a $\pm$10 m/sec effect. This is not a negligible effect, in fact it is equal to the maximum error, but it is a systematic effect which can be corrected in ground processing.

   1.3. The previous "symmetric" backgammon anode had a full 8 mil offset, which led to a large effect. The current design has a 1 mil offset. It is possible to reduce this further, by "twisting" the geometry, but it adds to fabrication difficulties. The recommendation here is to accept the 1 mil variation and correct for the effect in the data analysis software on the ground.

2. For 15 and 20 mils there is no measurable aliasing with very little random error. The azimuthal measurements have a spreading of well under 0.05°. Once the systematic distortion mentioned above is removed, the radial measurements have a spreading of well under 0.1 mil, i.e. 0.02°. These residual fluctuations could be numerical artifacts.

3. For a 10 mil spot radius, aliasing is visible. The worst-case azimuthal aliasing is $\pm 0.5°$ and occurs at an azimuth of 180°. Small fluctuations in total charge are observed, only 0.1% but indicating that a measurable fraction of the charge cloud is being lost. The period is equal to the wedge-wedge spacing, and since thermal spreading will smear an incident spot over several wedge pairs, this should contribute to a random spreading rather than any systematic effects.

4. The anode region where accurate results could be obtained depended on spot size and was worst for the 20 mil spot. For an anode going from 260 to 530 mils, the region where the response was extremely linear was limited to 310 to 470 mils. Outside of this region, systematic distortions in both elevation and azimuth were observed.

It should be noted that the model assumes that the wedge boundaries are very accurately known. Any real-world fabrication process will cause distortions in the wedge boundaries, steps or "waves" or something. This is likely to cause broadening beyond that computed here.

3.8 Anode Optimization

We can now consider the question of how we optimize the anode. To begin with, this analysis indicates that the current anode design will do fine. It will deliver the necessary resolution. Note that no consideration has been given to the bar region here, but assuming it can be handled satisfactorily, this design meets all the requirements, and can certainly be fabricated. Some noteworthy observations are as follows:

(i) we cannot make the wedge pairs any larger than they now are, or aliasing will become significant.

(ii) we don't want to make any feature sizes or spacings smaller than we currently have, or fabrication will either become more difficult due to increased tolerances or will lead to more fluctuations due to changing wedge sizes.

(iii) it has been proposed that the single azimuthal cycle pattern be replaced with two or more cycles. Adding more cycles adds considerably to circuit complexity. In fact, it is not clear that we can put two or four times the analog electronics on the board. Further, this analysis shows that this is not required to obtain the needed resolution, as a single cycle does just fine.

(iv) it has been proposed that interstitial elements be inserted between the wedges. If the 1 mil feature size is kept, it is clear that these additional elements would increase the radial offset between wedges, and consequently increases the radial aliasing with azimuth for all events. This will also increase the dead area fraction, thus increasing azimuthal aliasing with radius for the smaller events. This analysis shows that it is not required.

One change that is reasonable to make is to increase the width of the "tail", from 1 mils to say 1.5 or 2 mils. This will have essentially had no impact on the elevation measurement, which is determined from the number of anode pairs. For the azimuthal measurement, the radial offset between the centers increases somewhat, thereby increasing the radial aliasing with azimuth. The noise σ_A will be unchanged. However, the range of A will, in general, decrease. How much it decreases with tail width is difficult to compute, but it clearly does decrease (consider the limit of the tail equal to the head). The signal to noise ratio thus decreases - we lose the ability to accurately measure azimuth.

The only reason to do this would be if fabrication tolerances make it uncertain that we will get accurate, 1 mil tails.

Another change that can be made is to add additional wedge pairs outside of the existing 260 to 530 mil radial range. This would increase the radial range with an accurate linear response, thereby improving signal to noise ratio. This might be a good idea.

4.0 COUNT RATE EFFECTS

The essential question to be answered here is: how well does DIDM-3 determine the location of the centroid of the distribution, in the measurement time interval? To formulate an answer, the following factors were considered: (i) statistical fluctuations; (ii) low count rate considerations; (iii) high count rate considerations.

4.1 Count Rate Calculations

The MATHCAD worksheet showing the factors that go into determining the count rate in the instrument's sensor assembly, as well as, plots of MCP Count rate vs. Density, are shown in color plots in Figure 2. Plots for aperture sizes that have previously been considered for use in the instrument, (namely 1, 3 and 6 thousandth of an inch) are shown. The calculation assumes the same sensor assembly configuration as in DIDM-2, but uses one less grid screen. Also, for lack of a definitive number, MCP efficiency was assumed to be 10%. It is apparent from the results that for the smallest aperture size at the highest density, MCP count rate is 8×10^5 /sec. On the other end, for the largest size aperture at the lowest density, the count rate is 300 /sec. This suggests that with these two sizes, the sensor assembly can inherently handle an incident rate > 1×10^6 /sec, since designing electronics to handle this dynamic range is not terribly difficult.

It is also seen however, that with the 1 mil aperture at the lowest density, the count rate is about 8 /sec, while the 6 mil aperture at the highest density achieves a rate of 3×10^7 /sec. There is consequently five orders of magnitude in dynamic range for any one aperture size. This makes it unlikely that the instrument can be built with only a single aperture, as achieving such a dynamic range capability in the detection electronics is very challenging task.

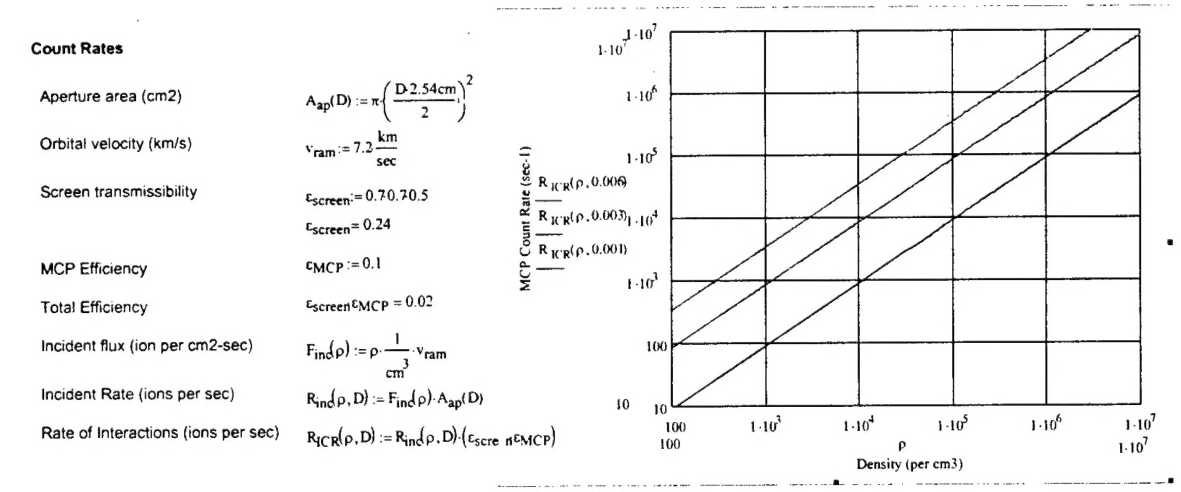

Figure 2. MCP Count Rate vs. Density

4.2 Low Count Rate Considerations

Inherently, the accuracy of DIDM instrument measurements is statistically limited in low flux environments. An essential question to answer in this context is: what is the minimum number of counts necessary to achieve the specified 25 m/sec drift measurement accuracy. The analysis of this subject was carried out by the Principal Investigator at AFRL, who determined the number to be □ 5,000 counts. To illustrate a practical consequence of this number, consider that to achieve a measurement resolution within 10 km (1.4 sec acquisition period) the ambient density must be greater than: (5,000 cts)/(1.4 sec) = 3,600 sec^{-1} $\Rightarrow$ $\rho > 1.2x10^3$ cm^{-3} (for 6 mil aperture). It is clearly seen therefore that measurement precision and resolution are linked parameters for the instrument, and the parameter space over which the desired accuracy for both is achievable could be significantly restricted. For example, if better measurement resolution is desired, say 25m/s at 16 Hz rate (□ 0.5 km), this leads to: 5,000 cts * 16 sec^{-1} = $8.0x10^4$ cps $\Rightarrow$ $\rho > 2.9x10^4$ cm^{-3} (for 6 mil aperture). To achieve higher resolution, correspondingly higher density regimes are necessary. If environmental conditions are such that the ambient ion density is adequate, there is no concern, but if this is not the case, the desired resolution will not be achieved. Of course, the option of employing a larger aperture size exists, but there are associated implementation issues to be considered here as well.

4.3 High Count Rate Pile-up Considerations

It is also useful to consider how well the DIDM instrument functions in high-count regimes. Particularly in instances when the count rate meets or exceeds the throughput capability of the electronics. DIDM-3 uses a centroiding technique to find the location of a single event charge cloud, which is distributed over the anode surface. Pile-up occurs when two charge clouds are coincident on the anode surface, and when this occurs the instrument finds the centroid of the total charge distribution. The net impact has bearings on the determined ion temperature and velocity. To get a sense of the consequences of pile-up within the instrument, the effect was simulated and the impact on input coordinate determination assessed. A summary of the process is as follows:

- model starts with an incident drift direction and temperature
- computes incident ion position with gaussian random number generator
- for each, computes charges q_{x1}, q_{x2}, q_{x3}, q_{x4}
- compute probability of pile-up with uniform random number generator
- if pile-up occurs, then combines charges weighted by gaussian gain
- computes az and el of resulting charge cloud
- computes centroid and total rms spreading in az and el

$$El_{dis} := rnorm(npts, El_{inc}, El_{rms}) \qquad p := runif(npts, 0, 1)$$

$$Az_{dis} := rnorm(npts, Az_{inc}, Az_{rms}) \qquad F := 0.25$$

$$G_{dis} := rnorm(npts, G_{mean}, G_{rms}) \qquad pur_i := \Phi(F - p_i)$$

$$Az_{pur_i} := Az_{der}(X1_{dis_i} + X1_{pu_i} \cdot pur_i, X2_{dis_i} + X2_{pu_i} \cdot pur_i, X3_{dis_i} + X3_{pu_i} \cdot pur_i, X4_{dis_i} + X4_{pu_i} \cdot pur_i)$$

One result of pile-up is that there is the apparent effect of less spreading over anode surface per incident event. This mimics the effect of an ambient population with colder temperature distribution, and introduces a systematic error in position determination. AFRL has determined that knowing the actual temperature with a resolution of 10% leads to acceptable drift errors, so correspondingly an rms spreading error of 5% or better is acceptable for the extent of 'spreading' in incident elevation and

azimuthal angle determinations. Using this criterion, the simulation shows that a pile-up fraction of 25% is the maximum acceptable. Table 3 shows the pile-up fraction at three temperatures for elevation and azimuth.

A plot showing histogram of counts versus elevation without pile-up and with 25% pile-up, for T=1,000 K is seen in Figure 3.

Table 3. Pile-up Fraction at 3 Temperatures for Elevation and Azimuth

	1000 K		2000 K		5000 K	
Piled Up Fraction	Elevation	Azimuth	Elevation	Azimuth	Elevation	Azimuth
	Degrees rms					
0%	5.8	20.4	8.0	27.8	12.6	39.8
10%	5.7	19.8	7.8	27.0	12.2	39.0
20%	5.5	19.6	7.6	26.3	11.9	38.1
30%	5.4	19.2	7.4	25.6	11.7	37.4
40%	5.2	18.6	7.3	24.8	11.3	36.2
50%	5.0	18.0	7.0	24.2	11.0	35.0
100%	4.3	14.9	5.9	20.2	9.2	29.1
	Normalized					
0%	100%	100%	100%	100%	100%	100%
10%	99%	97%	98%	97%	97%	98%
20%	**95%**	**96%**	**95%**	**95%**	**94%**	**96%**
30%	93%	94%	93%	92%	93%	94%
40%	90%	91%	91%	89%	90%	91%
50%	87%	88%	88%	87%	87%	88%
100%	75%	73%	74%	73%	73%	73%

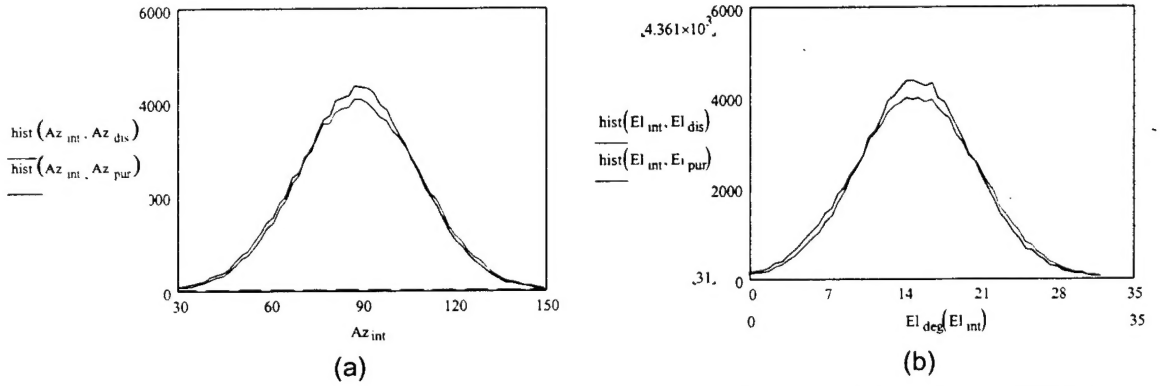

Figure 3. Histogram of: (a) Counts vs. Azimuth; (b) Counts vs. Elevation; without pile-up (in blue) and with 25% pile-up (in red), for T=1,000 K

The probability of pile-up was next determined from the following MATHCAD formulation:

A summary of aperture diameter, useful count rate, required minimum ambient density and 25% pile-up threshold is provided in Table 4.

$$P_{nopileup}(R) := \left(e^{-R\cdot\tau_{FW}}\right)^2$$

Probability of a pulse w/o pile-up (Knoll, p 612)

$$OCR_{nopileup}(R) := P_{nopileup}(R)\cdot R$$

Rate of "clean" pulses, w/o pile-up. This equals the probability times the rate of incoming pulses

$$P_{purfail}(R) := \left(1 - e^{-R\cdot\tau_{fast}}\right)\cdot e^{-2\cdot R\cdot\tau_{FW}}$$

Probability that PUR will fail, ie that pulses occur within the "fast" window times probability they are not rejected by PUR

$$R_{purfail}(R) := R\cdot P_{purfail}(R)$$

Rate at which PUR fails

$$F_{bad}(R) := \frac{P_{purfail}(R)}{P_{nopileup}(R) + P_{purfail}(R)}$$

Fraction of pulses passes by PUR which are bad

$$OCR_{PURpass}(R) := R_{purfail}(R) + OCR_{nopileup}(R)$$

Rate at which digitizer is triggered, ie the sum of the "good" pulses w/o PU and the "bad" pulses where PUR failed to preject a PU

$$OCR_{driftnogate}(R) := OCR_{nonparalyzable}\left(OCR_{PURpass}(R), \tau_{dig}\right)$$

Table 4. Count Rate Effect Summary

Aperture diameter	6 mil	3 mil	1 mil
5,000 cts at 2 Hz	$3.2\text{x}10^3$	$1.3\text{x}10^4$	$1.1\text{x}10^5$
5,000 cts at 16 Hz	$2.9\text{x}10^4$	$1.2\text{x}10^5$	$1.1\text{x}10^6$
Pile-up = 25%	$1.3\text{x}10^6$	$5.0\text{x}10^6$	$4.5\text{x}10^7$